Acquisition Geometry-aware Focal Deblending

Kontakis, Apostolos; Wu, S.; Verschuur, Eric

DOI
10.3997/2214-4609.201601411

Publication date
2016

Document Version
Final published version

Published in
78th EAGE Conference and Exhibition 2016, Vienna, Austria

Th P4 05

Acquisition Geometry-aware Focal Deblending

A. Kontakis* (Delft University of Technology), S. Wu (Delft University of Technology) & D.J. Verschuur (Delft University of Technology)

SUMMARY

The applicability of a deblending method is directly related to acquisition parameters, such as source and detector locations. We formulate focal deblending in two alternative ways. In the first case, the double focal transform is used, which relies on a well-sampled source and detector dimension. In the second case, the single-sided focal transform is used, which does not depend on a well-sampled source dimension. Comparing the deblending results, we find that although the double focal transform is superior, blending noise can be significantly attenuated using the single-sided focal transform, which allows application to more practical acquisition geometries. By combining with shot repetition, the deblending result can be further improved.

Introduction

Simultaneous shooting, also known as blending, has been proposed as a method for speeding up seismic acquisition and/or sampling the seismic wavefield more comprehensively, see e.g. Berkhout (2008). This is achieved by allowing the wavefields generated by each source to overlap, the overlap being controlled by a chosen code – the blending code. The price one has to pay for realizing the benefits of blending, is the need for source wavefield separation, alternatively referred to as deblending. This has to be of high enough quality such that subsequent processesing is not harmed.

Separating the interfering source wavefields is a challenging process, because of the inherent underdetermined nature of the problem. There is a wealth of methods that have been proposed to attack the problem. These range from coherency-based FK filtering (Mahdad et al., 2011), median-based filtering (Huo et al., 2012; Gan et al., 2015; Zhan et al., 2015), to sparsity-based methods using Radon transforms (Ayeni et al., 2011; Haacke et al., 2015; Ibrahim and Sacchi, 2013), curvelets (Lin and Herrmann, 2009; Wason et al., 2011) and seislets (Chen, 2015). Another approach is to use rank-reduction techniques (Wason et al., 2014; Cheng and Sacchi, 2015), exploiting the fact that blending increases the rank of certain data subsets.

Kontakis and Verschuur (2014) proposed a sparsity-based method for deblending, which used the double focal transform, utilizing prior knowledge about the subsurface, in the form of an approximate velocity model, in order to constrain the deblending inversion. A downside of the double focal transform is its requirement of dense source and detector sampling. Therefore, an interesting question is how the focal transform can be modified to accomodate for challenging geometries e.g. in cases where the source dimension is not sampled densely enough, or in subsets of a big 3D survey. Therefore, we examine two different ways to implement the focal transform, each one with different requirements when it comes to source sampling. Another question that we aim to address is whether focal deblending can be effectively combined with shot repetition (Wu et al., 2015) in order to enhance the quality of the deblending result.

Method and Theory

For the following discussion, we assume that an uppercase bold letter denotes a monochromatic frequency slice of a dataset or operator, following the notation found in Berkhout (1982). Then, the deblending problem can be posed as follows: given a blended dataset $\mathbf{P}_{\text{bl}}$ and a blending operator $\mathbf{\Gamma}$, find the unblended dataset $\mathbf{P}$ that satisfies

$$\min_{\mathbf{P}} \left\{ \sum_{\omega} ||\mathbf{P}_{\text{bl}} - \mathbf{P}\mathbf{\Gamma}||_{\text{F}}^2 \right\}, \tag{1}$$

subject to any desired additional constraints on $\mathbf{P}$. We use $||\mathbf{X}||_{\text{F}}^2 = \sum_m \sum_n |X_{mn}|^2$ to denote the squared Frobenius norm of matrix $\mathbf{X}$, X_{mn} being its (m,n)-th element. Placing additional contraints on (1) is a necessity, because $\mathbf{\Gamma}$ is a tall matrix, which makes the deblending problem underdetermined. Without additional constraints (1) has no unique solution.

Our approach to constraining (1) is to use prior knowledge about the subsurface in the form of an approximate velocity model and a number of depth levels, where the strongest reflectors lie. This approximate information is often available, e.g. in timelapse acquisition, and it can be used to provide a sparse representation of $\mathbf{P}$. The expected sparsity can be used to effectively constrain (1). The vehicle for achieving this sparse representation of $\mathbf{P}$ is the multi-level focal transform, assuming that $\mathbf{P}$ is compressed in the focal domain.

The focal transform can be defined in different ways, depending on what suits better the acquisition geometry. When the source and receiver dimension are well sampled, it is possible to use the double focal transform (Berkhout and Verschuur, 2010; Kutscha et al., 2010; Kutscha and Verschuur, 2012). In this case, K pairs of wavefield extrapolation operators $\mathbf{W}_k^+$ and $\mathbf{W}_k^-$ are created, using the velocity model. $\mathbf{W}_k^+$ extrapolates a wavefield the surface to depth level z_k. $\mathbf{W}_k^-$ does the reverse operation, which is to extrapolate a wavefield from a depth level z_k to the surface. Each pair of operators defines a focal subdomain, $\delta\mathbf{X}_k$, which contains "compressed" information about reflection events originating from z_k and its vicinity. The relationship between $\mathbf{P}$ and $\delta\mathbf{X}_k$ is given by

$$\mathbf{P} = \sum_{k=1}^{K} \mathbf{W}_k^- \delta\mathbf{X}_k \mathbf{W}_k^+. \tag{2}$$

Equation (2) is the inverse double focal transform. Using (2) it is possible to recover the wavefield recorded at the surface from the focal subdomains. The adjoint operation takes the surface data $\mathbf{P}$ and focuses it at depth level z_k:

$$\delta\mathbf{X}_k \approx \mathbf{W}_k^{-\mathrm{H}}\mathbf{P}\mathbf{W}_k^{+\mathrm{H}}, \qquad k = 1,\ldots,K. \tag{3}$$

Here $\mathbf{W}^{\mathrm{H}}$ denotes the conjugate transpose of $\mathbf{W}$. It can be easily seen that operators $\mathbf{W}_k^{+}$ and $\mathbf{W}_k^{-}$ act on both source and detector dimension in order to focus the data. In 3D acquisition scenarios, achieving good sampling of both x and y dimensions for sources and detectors can be very challenging. It is therefore useful to investigate alternative formulations that can provide focusing, without having to act on both source and detector dimensions. A way to accomplish this is to work with "two-way" operators $\mathbf{G}_k$ (Berkhout and Verschuur, 2006). Then (2) becomes

$$\mathbf{P} = \sum_{k=1}^{K} \mathbf{G}_k \delta\mathbf{X}_k, \tag{4}$$

which we will refer to as the single-sided focal transform. The content of $\delta\mathbf{X}_k$ now can be interpreted as being the portion of a source wavefield that gets reflected at depth z_k and its vicinity. The adjoint now becomes

$$\delta\mathbf{X}_k \approx \mathbf{G}_k^{\mathrm{H}}\mathbf{P}, \qquad k = 1,\ldots,K. \tag{5}$$

The focusing operation that takes place in (5) now acts only on the receiver dimension and is also cheaper to compute, needing half the number of matrix-matrix operations to be computed. A major difference between (2) and (4) is how blending noise is mapped to the focal domain. When using (5) the blending noise is also focused, unlike (3), where blending noise does not focus. This makes using (4) more difficult for high quality deblending. This problem can be, to some extent, mitigated by using weights in the focal domain.

Focal deblending can also benefit from using more complex blending codes, such as the shot repetition method discussed in the introduction. When shot repetition is employed in the survey, the source fires multiple times per shot location, with small time delays. Each element (m,n) of $\mathbf{\Gamma}$ is given then by

$$\Gamma_{mn} = \begin{cases} \sum_{l=1}^{L} e^{-j\omega\tau_{mnl}}, & \text{if shot } m \text{ is blended in the } n\text{th blended shot gather} \\ 0, & \text{if shot } m \text{ is not blended in the } n\text{th blended shot gather,} \end{cases} \tag{6}$$

where L is the number of shot repetitions, and τ_{mnl} the time delays. Note that for $L = 1$, (6) becomes a standard random time delay code. As shown in Wu et al. (2015), the shot repetition code for each shot is designed such that its autocorrelation is spiky and its crosscorrelation with the codes of other shots is small for every lag. As a result, the signal to be extracted is boosted compared to the blending noise. This makes blending noise less likely to be part of the deblended result.

Returning to the problem of constraining (1), we can make use of the focal representation of the data and apply sparsity-promoting regularization there, exploiting the expected sparseness of the solution. This can be done by inserting (2) in (1), which yields

$$\min_{\delta\tilde{\mathbf{X}}_k} \left\{ \sum_{\omega} ||\mathbf{P}_{\mathrm{bl}} - \sum_{k=1}^{K} \mathbf{W}_k^{-}\delta\mathbf{X}_k\mathbf{W}_k^{+}\mathbf{\Gamma}||_{\mathrm{F}}^2 + \varepsilon \sum_{t}\sum_{k=1}^{K} ||\delta\tilde{\mathbf{X}}_k||_{\mathrm{V,S}} \right\}, \tag{7}$$

or,

$$\min_{\delta\tilde{\mathbf{X}}_k} \left\{ \sum_{\omega} ||\mathbf{P}_{\mathrm{bl}} - \sum_{k=1}^{K} \mathbf{G}_k\delta\mathbf{X}_k\mathbf{\Gamma}||_{\mathrm{F}}^2 + \varepsilon \sum_{t}\sum_{k=1}^{K} ||\delta\tilde{\mathbf{X}}_k||_{\mathrm{V,S}} \right\}, \tag{8}$$

when "two-way" focusing operators are used. $\delta\tilde{\mathbf{X}}_k$ is the kth focal subdomain in the time domain and $||\mathbf{X}||_{\mathrm{S}} = \sum_m\sum_n |V_{mn}X_{mn}|$, $V_{mn} > 0$, denotes the weighted sum-norm. The vectorized form of (7) and (8) is essentially a basis pursuit denoising problem, which can be solved by solvers such as SPGL1 (van den Berg and Friedlander, 2007, 2008). It is also possible to combine the focal transform with other transforms, such as the linear Radon transform, as shown in Kontakis and Verschuur (2015).

Examples

The method is tested using a numerically blended 2D marine line from a North Sea field dataset. The dataset consists of 151 sources and detectors, with a source/detector spacing of 12.5m. The time sampling interval is 8ms. Interpolation and the reciprocity principle were used in order to reconstruct the

near offset data (Kabir and Verschuur, 1995). Surface-related multiples were also removed. The blending factor used is 2. Thirteen focal operators were used, that were constructed through NMO analysis. Their zero offset times were where ranging from 0.34s to 1.44s. Both the simple time delay and shot repetition codes used time delays from 0.1s to 0.5s.

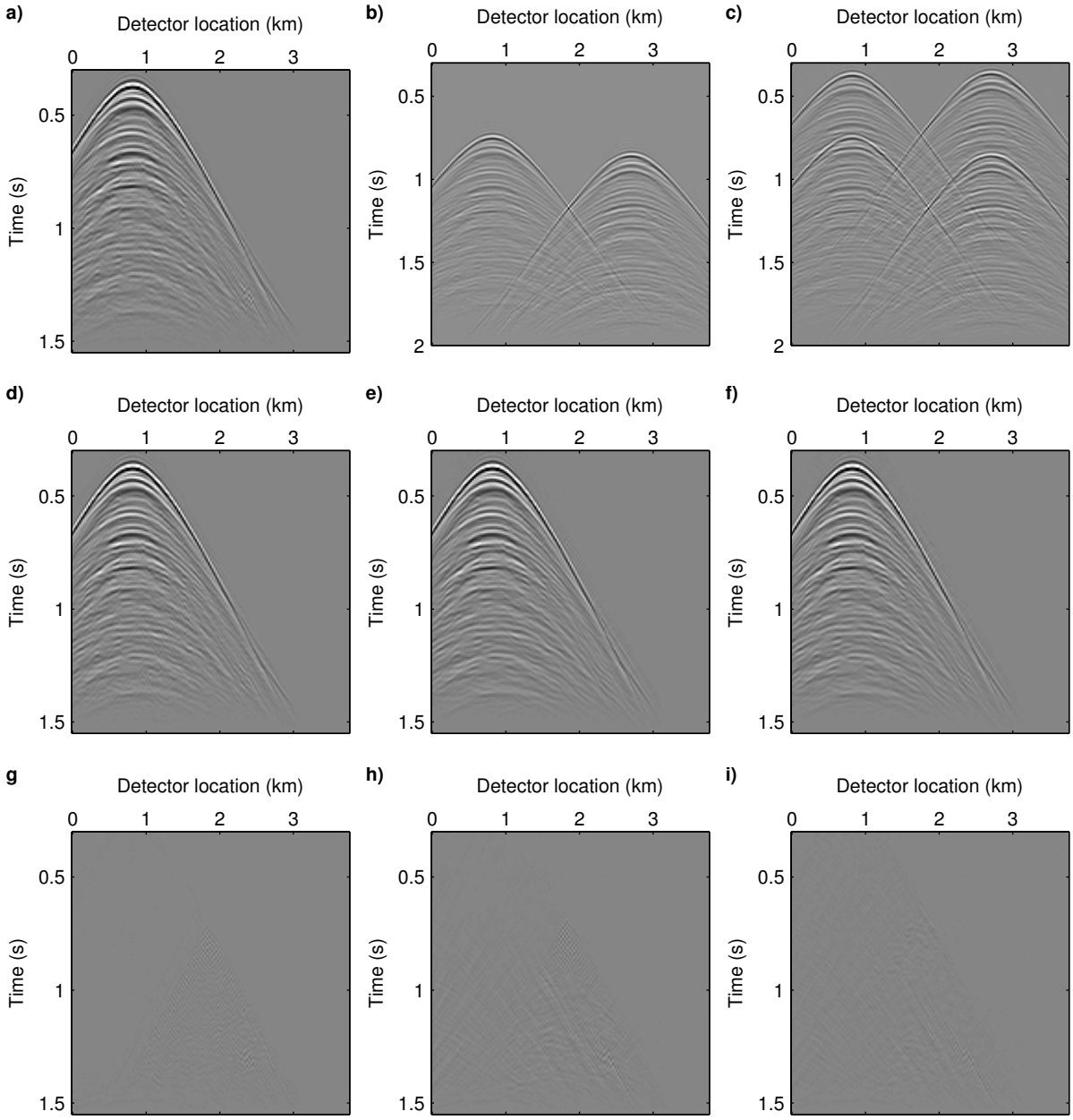

Figure 1 *a) Original field dataset, b) numerically blended data (time delays), c) blended data (shot repetition). Deblended result: d) double focal transform, time delays, e) single-sided focal transform, time delays, f) single-sided focal transform, shot repetition. Error section: g) double focal transform, time delays, h) single-sided focal transform, time delays, i) single-sided focal transform, shot repetition.*

The results shown in Figure 1 were calculated for three different cases: i) deblending using the double focal transform and a simple random time delay code, ii) using the single-sided focal transform and the same simple-random time delay code as the previous example and iii) using the single-sided focal transform and shot repetition with each shot repeated 2 times. They are assessed using a quality metric $Q = 10\log_{10}(\sum_t ||\tilde{\mathbf{P}}_{\text{ideal}}||_{\text{F}}^2 / \sum_t ||\tilde{\mathbf{P}}_{\text{ideal}} - \tilde{\mathbf{P}}||_{\text{F}}^2)$. Here, $\tilde{\mathbf{P}}_{\text{ideal}}$ and $\tilde{\mathbf{P}}$ are the ideal, noise-free data and the deblended data respectively, in the time domain. For the example shown above and the three cases examined, $Q_{i)} = 18.50$ dB, $Q_{ii)} = 16.46$ dB and $Q_{iii)} = 18.17$ dB.

Using the double focal transform yields better results, however it needs well-sampled source and detector

dimensions. Using the single-sided focal transform relaxes the requirement for a well-sampled source dimension, at the expense of deblending quality, as expected. Still, however, the deblended dataset has minimal amplitude differences compared to the original noise-free data. Shot repetition improves the result, due to the ability of the repeated shots to boost the signal-to-noise ratio.

Conclusions

We showed that focal deblending can be redefined in different ways, in order to perform deblending even in cases where the shot dimension is not well-sampled, which could be difficult to handle with methods that rely on blending noise incoherency. Also, relaxing the requirement for a fully sampled wavefield paves the path for the development of focal operators that are tailored to specific acquisition geometries, which can be useful when handling big 3D blended surveys. When employed, shot repetition proves to also enhance the separation quality.

Acknowledgements

The authors would like to thank sponsors of the Delphi consortium for their support as well as the authors of the SPGL1 solver for making it publicly available.

References

Ayeni, G., Almomin, A. and Nichols, D. [2011] On the separation of simultaneous source-data by inversion. *81st SEG Annual International Meeting*, Expanded Abstracts, 20–25.

van den Berg, E. and Friedlander, M.P. [2007] SPGL1: A solver for large-scale sparse reconstruction. Http://www.cs.ubc.ca/labs/scl/spgl1.

van den Berg, E. and Friedlander, M.P. [2008] Probing the Pareto frontier for basis pursuit solutions. *SIAM Journal on Scientific Computing*, **31**(2), 890–912.

Berkhout, A.J. [1982] *Seismic migration, imaging of acoustic energy by wave field extrapolation, A: Theoretical aspects*. Elsevier (second edition).

Berkhout, A.J. [2008] Changing the mindset in seismic data acquisition. *The Leading Edge*, **27**(7), 924–938.

Berkhout, A.J. and Verschuur, D.J. [2006] Focal transformation, an imaging concept for signal restoration and noise removal. *Geophysics*, **71**(6), A55–A59.

Berkhout, A.J. and Verschuur, D.J. [2010] Parameterization of seismic data using gridpoint responses. *80th SEG Annual International Meeting*, Expanded Abstracts, 3344–3348.

Chen, Y. [2015] Deblending by iterative orthogonalization and seislet thresholding. *85th SEG Annual International Meeting*, Expanded Abstracts, 53–58.

Cheng, J. and Sacchi, M.D. [2015] A fast rank-reduction algorithm for 3D deblending via randomized QR decomposition. *85th SEG Annual International Meeting*, Expanded Abstracts, 3830–3835.

Gan, S., Wang, S., Chen, X. and Chen, Y. [2015] Deblending using a structural-oriented median filter. *85th SEG Annual International Meeting*, Expanded Abstracts, 59–64.

Haacke, R., Hampson, G. and Golebiowski, B. [2015] Simultaneous shooting for sparse OBN 4D surveys and deblending using modified Radon operators. *77st EAGE Conference & Exhibition*, Extended Abstracts, We N101 08.

Huo, S., Luo, Y. and Kelamis, P.G. [2012] Simultaneous sources separation via multidirectional vector-median filtering. *Geophysics*, **77**(4), V123–V131.

Ibrahim, A. and Sacchi, M.D. [2013] Simultaneous source separation using a robust Radon transform. *Geophysics*, **79**(1), V1–V11.

Kabir, M.M.N. and Verschuur, D.J. [1995] Restoration of missing offsets by parabolic Radon transform. *Geophysical Prospecting*, **43**(3), 347–368.

Kontakis, A. and Verschuur, D.J. [2014] Deblending via sparsity-constrained inversion in the focal domain. *76th EAGE Conference & Exhibition*, Extended Abstracts, Th ELI2 02.

Kontakis, A. and Verschuur, D.J. [2015] Deblending via a hybrid focal and linear Radon transform. *77th EAGE Conference & Exhibition*, Extended Abstracts, We N101 02.

Kutscha, H. and Verschuur, D.J. [2012] Data reconstruction via sparse double focal transformation: An overview. *Signal Processing Magazine, IEEE*, **29**(4), 53–60.

Kutscha, H., Verschuur, D.J. and Berkhout, A.J. [2010] High resolution double focal transformation and its application to data reconstruction. *80th SEG Annual International Meeting*, Expanded Abstracts, 3589–3593.

Lin, T.T.Y. and Herrmann, F.J. [2009] Designing simultaneous acquisitions with compressive sensing. *71st EAGE Conference & Exhibition*, Extended Abstracts, S006.

Mahdad, A., Doulgeris, P. and Blacquière, G. [2011] Separation of blended data by iterative estimation and subtraction of blending interference noise. *Geophysics*, **76**(3), Q9–Q17.

Wason, H., Herrmann, F.J. and Lin, T.T.Y. [2011] Sparsity-promoting recovery from simultaneous data: a compressive sensing approach. *81st SEG Annual International Meeting*, Expanded Abstracts, 6–10.

Wason, H., Kumar, R., Herrmann, F.J. and Aravkin, A.Y. [2014] Source separation via SVD-free rank minimization in the hierarchical semi-separable representation. *84th SEG Annual International Meeting*, Expanded Abstracts, 120–126.

Wu, S., Blacquière, G., and van Groenestijn, G.J. [2015] Shot repetition: an alternative approach to blending in marine seismic. *85th SEG Annual International Meeting*, Expanded Abstracts, 120–126.

Zhan, C., Malik, R., Specht, J., Liu, Z. and Teixeira, D. [2015] Deblending of continuously recorded OBN data by subtraction integrated with a median filter. *85th SEG Annual International Meeting*, Expanded Abstracts, 4673–4677.